

07,11,12

Parity effect — symmetry of n-alkanes molecules

© A.K. Borisov, V.A. Marikhin, V.M. Egorov

Ioffe Institute,
St. Petersburg, Russia

E-mail: borisov.ak@mail.ioffe.ru

Received March 7, 2024

Revised March 7, 2024

Accepted March 27, 2024

The features of phase transitions in the homologous series of normal alkanes of different parities have been studied. The real values of thermodynamic parameters were obtained as a result of eliminating the methodological errors of differential scanning calorimetry. The presence of a parity effect in the homologous series of n-alkanes was revealed both in the behavior of the thermodynamic parameters of phase transitions and in the process of structural rearrangement of crystallographic packing during the solid-solid phase transition, caused by different symmetries of n-alkane molecules.

Keywords: n-alkanes, molecular crystals, molecular packing, symmetry, phase transitions, differential scanning calorimetry, parity effect.

DOI: 10.61011/PSS.2024.05.58504.46

1. Introduction

Development of a new method of energy conversion, transportation and storage due to using phase change materials (PCM) is one of the promising development areas of the „green energy“. Wide use of PCM makes it possible to avoid heat sources whose operation requires limited energy resources because PCM can convert (accumulate, store and release) thermal energy flows from various sources using inherent thermal effects as a result of phase transitions. Long-chain molecular n-alkane crystals are one of the most promising materials used as PCM due to their high energy efficiency, flexibility of thermodynamic properties and availability [1–3]. N-alkanes and their mixtures used as PCM help create comfortable living conditions for people in a temperature range from -40 to 70°C . On the other hand, monodisperse n-alkanes are convenient models used to identify the nature of phase transitions and establish the „structure–property“ patterns owing to the absence of structural and conformational defects.

Our previous studies [4,5] investigated thermodynamic properties of some n-alkanes and revealed dependences of the thermodynamic properties on parity of carbon atoms in the chain. To identify reliable dependences of properties on parity and establish the reasons for their appearance, this study investigates a wide homologous series of n-alkanes with varying the chain length (hexadecane $\text{C}_{16}\text{H}_{34}$, heptadecane $\text{C}_{17}\text{H}_{36}$, octadecane $\text{C}_{18}\text{H}_{38}$, nonadecane $\text{C}_{19}\text{H}_{40}$, eicosane $\text{C}_{20}\text{H}_{42}$, heneicosane $\text{C}_{21}\text{H}_{44}$, docosane $\text{C}_{22}\text{H}_{46}$, tricosane $\text{C}_{23}\text{H}_{48}$, tetracosane $\text{C}_{24}\text{H}_{50}$ and pentacosane $\text{C}_{25}\text{H}_{52}$) that have phase transition temperatures in the temperature range that is most suitable for applications: $\Delta T \approx 10\text{--}50^{\circ}\text{C}$. Thus, examination of this homologous series is used to solve fundamental problems associated with

study of phase transition kinetics in n-alkanes as well as practical problems associated with efficient application of n-alkanes as PCM.

2. Findings and discussion

The investigations were performed by the differential scanning calorimetry (DSC) method using DSK 500 Spetspribor (Russia) (for $\text{C}_{16}\text{H}_{34}\text{--}\text{C}_{20}\text{H}_{42}$) and Seiko DSC 6100 (Japan) (for $\text{C}_{21}\text{H}_{44}\text{--}\text{C}_{25}\text{H}_{52}$) in nitrogen atmosphere. Scanning rates varied in a wide range from 0.25 to 25 K/min. To reduce systematic errors, thermal resistance of samples and calorimetric capsules was minimized through low weight of samples (1–3 mg) and calorimetric capsules (16 mg). „Sigma-Aldrich“, high purity 99.5% monodisperse n-alkane powders were chosen as samples.

Temperature dependences of heat capacity in heating–cooling cycles were measured by the DSC method for each of the homologous series samples with scan rate variation. Figure 1 shows thermograms measured at 1 K/min. The figure shows that two peaks are observed for most n-alkanes in heating and cooling indicating a two-stage behavior of transition from the crystalline state to melt and back. However, for samples with even number of carbon atoms in the chain, merging of two heat capacity peaks into one is observed as the number decreases. Therefore, melting and crystallization peaks of short even n-alkanes are expected to combine both phase transformation stages resulting in distortion of peak shape. For odd n-alkanes with all chain lengths, two peaks in heating and two peaks in cooling are observed suggesting that there are different mechanisms of molecular restructuring during solid–melt phase transformation in n-alkanes with even and odd chain length.

For *n*-alkanes, it has been previously shown [6–8] that a low-temperature endothermic peaks $T_{\max 1}$ is caused by the structural phase transition taking place in the solid phase, while a high-temperature peak $T_{\max 2}$ is caused by the order–disorder transition followed by melting. When the sample is cooled from melt, sample crystallization corresponds to the exothermic peak $T_{\min 2}$, while structural solid-phase transition corresponds to $T_{\min 1}$. As shown in Figure 1, the temperature hysteresis effect is observed for both phase transitions, i.e. mismatch of phase transition (PT) temperatures in heating and cooling. Such hysteresis effect may be caused by physical aspects as well as by technical aspects associated with the features of the DSC method [9]. To find out the nature of hysteresis, a special method was used for all *n*-alkanes of interest [10] in order to remove the systematic error when recording a series of thermal images with wide variation of scan rates on the identical samples or on the same samples provided that PT reversibility is ensured.

Figure 2 shows an example of this method used for docosane $C_{22}H_{46}$. Experimental data is used to plot dependences $T_{\max, \min} = f(V^{1/2})$ that shall be linear when there are no structural changes. Extrapolation of these dependences to the zero scan rate gives technically undistorted values of PT temperatures. The figure shows that in extrapolation to the zero scan rate melting temperature $T_{\max 2}$ and crystallization temperature $T_{\min 2}$ coincided with each other $\Delta T_2 \approx 0$ K, including the error, while solid-phase transition temperatures in heating $T_{\max 1}$ and cooling $T_{\min 1}$ differ by $\Delta T_1 \approx 3.7$ K at the zero rate, i.e. true temperature hysteresis is observed.

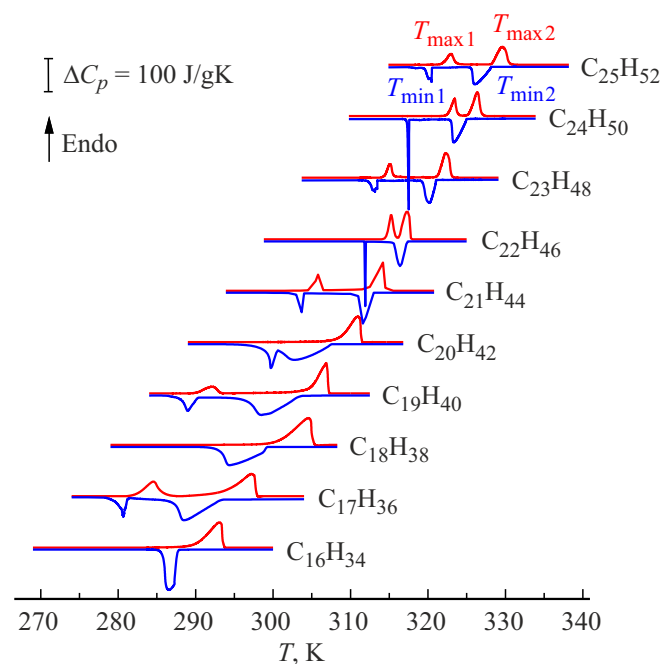


Figure 1. DSC curves of *n*-alkane homologous series heating (red lines) and cooling (blue lines) at a rate of 1 K/min.

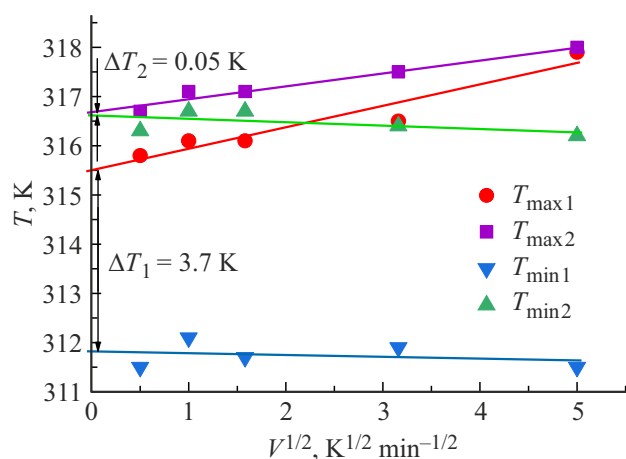


Figure 2. Method for finding true PT temperatures for docosane ($C_{22}H_{46}$).

Hence, it is suggested that the hysteresis effect occurs for the second peaks ($T_{\max 2}$, $T_{\min 2}$) only on the DSC thermograms due to technical factors, while the presence of the true hysteresis for the first peaks ($T_{\max 1}$, $T_{\min 1}$) is caused by physical factors. Thus, the presence of true temperature hysteresis allows assigning the solid-phase transition to first-order phase transitions (PT-1), while the melting–crystallization transition in *n*-alkanes by the absence of hysteresis and heat capacity peak shape may be assigned to second-order phase transitions (PT-2) similar to [9] for 1,22-docosanediol. It is important to note that true phase transition temperatures may be defined using the extrapolation method.

Phase transition temperatures calculated by the above-mentioned method for all *n*-alkanes are shown in Figure 3, *a*. PT-2 temperatures in heating ($T_{\max 2}$) and cooling ($T_{\min 2}$) coincide due to the absence of temperature hysteresis and rise smoothly as *n*-number of carbon atoms in the *n*-alkane chain increases, while PT-1 peak temperatures ($T_{\max 1}$ and $T_{\min 1}$) demonstrate „sawtooth“ dependences on parity *n*. The cause of this effect is associated with different molecular symmetry (trans and cis) even and odd *n*-alkanes and, accordingly, with their different packaging in the main cells and subcells depending on symmetry.

The effect of *n*-alkane parity on phase transformation temperatures was reported in [11,12], we also reported the effect of parity on PT-1 behavior kinetics [13]. Dependence of thermodynamic parameters on the chain length parity of *n*-alkane is known as the parity effect and is explained by different crystallographic packaging of even (trans) and odd (cis) molecules of *n*-alkanes into the main cells and subcells.

More detailed investigations have shown that not only PT temperatures, but also intervals between PT in heating ($\Delta T_{\max} = T_{\max 2} - T_{\max 1}$) and cooling ($\Delta T_{\min} = T_{\min 2} - T_{\min 1}$) differ significantly in even and odd *n*-alkanes. Figure 3, *b* shows that ΔT_{\max} and ΔT_{\min} in odd *n*-alkanes are several times higher than in even *n*-alkanes.

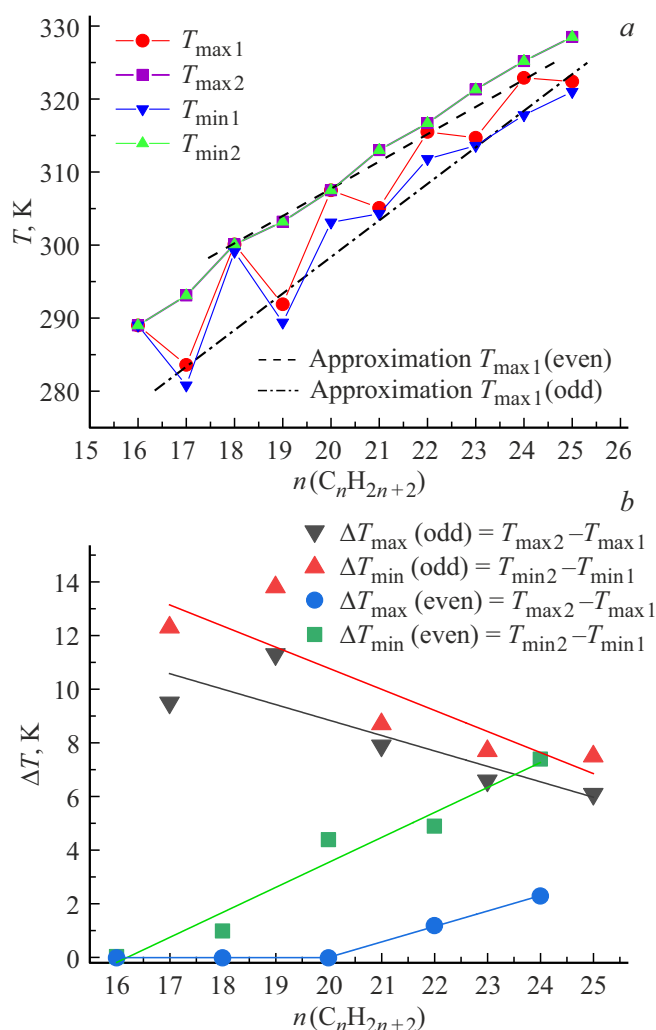


Figure 3. True PT temperatures of the homologous series of n-alkanes C_nH_{2n+2} (a) and dependences of temperature ranges between PT-1 and PT-2 in heating and cooling on the chain length (b).

Moreover, $\Delta T_{\max}(n)$ and $\Delta T_{\min}(n)$ demonstrate the opposite behavior of dependences with n growth, $\Delta T_{\max}(n)$ and $\Delta T_{\min}(n)$ grow in even n-alkanes and, on the contrary, decrease in odd n-alkanes. However, PT-2 temperatures do not depend on parity n and smoothly grow according to the dependence that has been established previously [14] and may be approximately considered as linear, which is also shown in Figure 3, a.

Thus, differences in ΔT_{\max} and ΔT_{\min} of even/odd n-alkanes are defined only by PT-1 position in which, as shown in [8,15,16], structural solid-phase transition from the initial subcell to an intermediate rotator phase takes place in $C_{16}H_{34}$ – $C_{25}H_{52}$ due to an increase in intermolecular distances as a result of thermal expansion, reduction of the Van der Waals interactions and occurrence of molecular rotation about their main axis with long-range order in molecule arrangement remained unchanged. Due to different symmetry of crystallographic cells, for

n-alkanes with even chain length — transition to phase RII (rhombohedral rotator) takes place, and for n-alkanes with odd chain length — initial transition to phase RI (orthorhombic rotator) takes place, however, then low-energy transition to phase RII occurs and, therefore, even and odd n-alkanes become equivalent for the next PT-2.

In short n-alkanes ($C_{16}H_{34}$, $C_{18}H_{38}$, $C_{20}H_{42}$), potential barrier of transition from the triclinic phase to the intermediate rotator phase is assumed to approach the barrier of transition from the triclinic phase directly into melt, therefore, the corresponding PT peaks merge on the DSC dependences during heating and the solid-phase transition cannot be isolated as it is. Whilst in odd n-alkanes, the potential barrier of transition from the orthorhombic phase to the intermediate rotator phase is obviously lower than the barrier of transition from the orthorhombic phase to melt and, therefore, the solid-phase transition occurs earlier than melting by several degrees. Figure 3, a shows that PT-1 temperature dependences growing from n have opposite slope with respect to PT-2 temperature dependences during heating in even (dashed line) and odd (dashed and dotted line) n-alkanes, therefore, the proportion of increase of the potential barrier for transition from the initial phase to the intermediate rotator phase (ΔE) decreases in each successive even n-alkane ($\Delta E_{n+1}/\Delta E_n < 1$), and increases in odd n-alkane ($\Delta E_{n+1}/\Delta E_n > 1$). For PT-1, the equivalent approach will be valid during cooling. Potential barrier of transition from the intermediate rotator phase to the equilibrium solid-state phase (triclinic phase in even n-alkanes and orthorhombic phase in odd n-alkanes) increases with growth of n . However, the proportion of barrier increase decreases in even and increases in odd n-alkanes. This assumption explains the opposite behavior of dependences of even/odd n-alkanes observed in Figure 3 b.

Investigation of hysteresis effects of PT-1 in n-alkanes is also of substantial interest. True temperature hysteresis values of PT-1 ($T_{\max 1} - T_{\min 1}$) depending on the n-alkane chain length and their second-order polynomial approximation are shown in Figure 4. It may be noted that an obvious difference in behavior of dependences on n for even and odd n-alkanes is also observed in this case. For even samples, hysteresis increase is observed as n grows from 16 to 24, while, for odd samples, hysteresis decrease is observed as n grows from 17 to 21, and then some growth is observed with further increase of n to 25.

Investigation of the nature of hysteresis effects is a vast problem and requires additional experimental and theoretical analysis, that will be performed in our future studies.

This study is focused on PT-1 behavior kinetics. Heat capacity peak shape is important because it is the one that contains the PT behavior data. To that end, PT-1 peak shapes both in heating and cooling have been analyzed for the first time. Figure 1 shows that solid-phase transition peaks are not distinguished against the melting peaks in heating for $C_{16}H_{34}$, $C_{18}H_{38}$ and $C_{20}H_{42}$ and against crystallization in cooling for $C_{16}H_{34}$ and $C_{18}H_{38}$. Therefore,

peaks of these coinciding transitions are not addressed below.

Figure 1 shows that PT-1 peaks have a quite large half width (1–2 K, i.e. „smeared“ in temperature), therefore, PT-1 in *n*-alkanes may be assigned to diffuse phase transitions (DPT). For analysis of heat capacity peaks of this type of phase transitions, diffuse phase transition theory has been developed [17–19]. The main idea of the DPT theory is in the fact that nucleation of the new phase develops according to a heterogeneous mechanism on various defects with generation of a phase boundary that is a specific feature of PT-1. Stable nuclei of the new phase, so-called elementary transformation volumes ω , are generated as a result of numerous fluctuations. The new phase boundary, as PT develops, moves forward by overlaying similar nanonuclei on each other. It is such stage-by-stage development of PT that results in PT smearing because generation of each new nanonuclei requires some additional change in energy due to a little temperature increase (decrease) ΔT , which also confirms the heterogeneous kinetics mechanism of PT-1.

According to the DPT theory, symmetric Λ -shaped heat capacity peaks are addressed. PT-1 peaks recorded experimentally have an asymmetric shape, therefore, separation into symmetric components may be performed using a method developed by us and described in detail in [20]. For all samples, the solid-phase transition peaks appeared to be divided into two symmetric Λ -shaped components. Therefore, we discuss the development of solid-phase transitions in all samples in two stages.

The theory calculates nanonuclei volumes ω at each stage using the analysis of peak shapes on $C_p(T)$. In [18], relation for the temperature dependence of heat capacity in diffuse phase transition was written as

$$\Delta C_p(T) = \frac{4\Delta C_m \exp\left[\frac{B(T-T_0)}{T_0}\right]}{\left[1 + \exp\left(\frac{B(T-T_0)}{T_0}\right)\right]^2}, \quad (1)$$

where T_0 is the PT-1 temperature, B is the athermic parameter, ΔC_m is the maximum heat capacity at $T = T_0$.

Athermic parameter B is a structurally sensitive quantity that defines smearing of transition over temperature. According to [17], B is correlated with an elementary transformation volume — new phase nuclei, as follows:

$$\omega = \frac{BkT}{\rho q_0} \quad (2)$$

where q_0 is the heat of transformation, ρ is the density, k is the Boltzmann constant.

Elementary transformation volumes were calculated using (1) and (2) for each of the PT-1 stages in the *n*-alkanes addressed in terms of the DPT theory in heating and, or the first time, in cooling. Elementary transformation volumes at the first PT-1 stage are of utmost interest because it is here where solid-phase transition is initiated. Nanonuclei volumes at the first stage also appeared to demonstrate general dependence on parity n , but differ in heating and

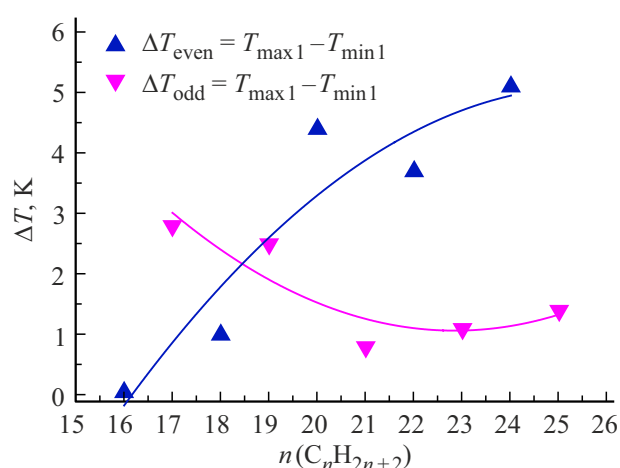


Figure 4. Dependence of the temperature hysteresis on the chain length in the homologous series of *n*-alkanes.

cooling: $\omega \sim 110 \text{ nm}^3$ in odd *n*-alkanes and $\omega \sim 240 \text{ nm}^3$ in even *n*-alkanes in heating (Figure 5, *a*); while in cooling $\omega \sim 120 \text{ nm}^3$ in odd *n*-alkanes and $\omega \sim 560 \text{ nm}^3$ in even *n*-alkanes (Figure 5, *b*).

At the second stage, considerable increase in nanonuclei volumes of odd *n*-alkanes takes place during heating. With increase in n , significant linear growth from 150 to 2800 nm^3 occurs as n increases (Figure 5, *c*), while no increase is observed in even *n*-alkanes and the first and second stage nanonuclei volumes appear to be approximately equal.

The PT-1 peaks in cooling in even *n*-alkanes is very narrow, resembling δ -function, however, it is still analyzable in terms of the DPT theory and one stage may be distinguished reliably. At the same time, the heat capacity peak shape in short odd *n*-alkane ($n = 17, 19$) is broadened and adequately symmetric, and, therefore, one Λ -shaped function was chosen for description within the framework of the theory. The second stage in heating was reliably distinguished only for the longest odd *n*-alkanes ($n = 21, 23, 25$) (Figure 5, *d*).

By knowing the elementary transformation volumes, the number of molecules included in the new phase nanonuclei may be estimated. These estimates in heating for the first PT-1 stage in the samples show that nanonuclei contain quite many molecules $N \sim 150\text{--}500$ depending on the sample. However, the second stage nanonuclei contain even more molecules that achieves $N = 6000$ in pentacosane. At the first stage in heating, nanonuclei appeared to contain ~ 2 times as many molecules ($N = 300\text{--}1100$ molecules) than at this stage in heating in the corresponding *n*-alkanes.

Second stages in cooling were successfully distinguished just for a few *n*-alkanes and in this case nanonuclei include $N \sim 300, 2500$ and 5000 molecules for $n = 21, 23$ and 25 , respectively. In this case, correlation with the heating process is not observed, however, as n rows, a very significant linear growth of nanonuclei volumes is observed

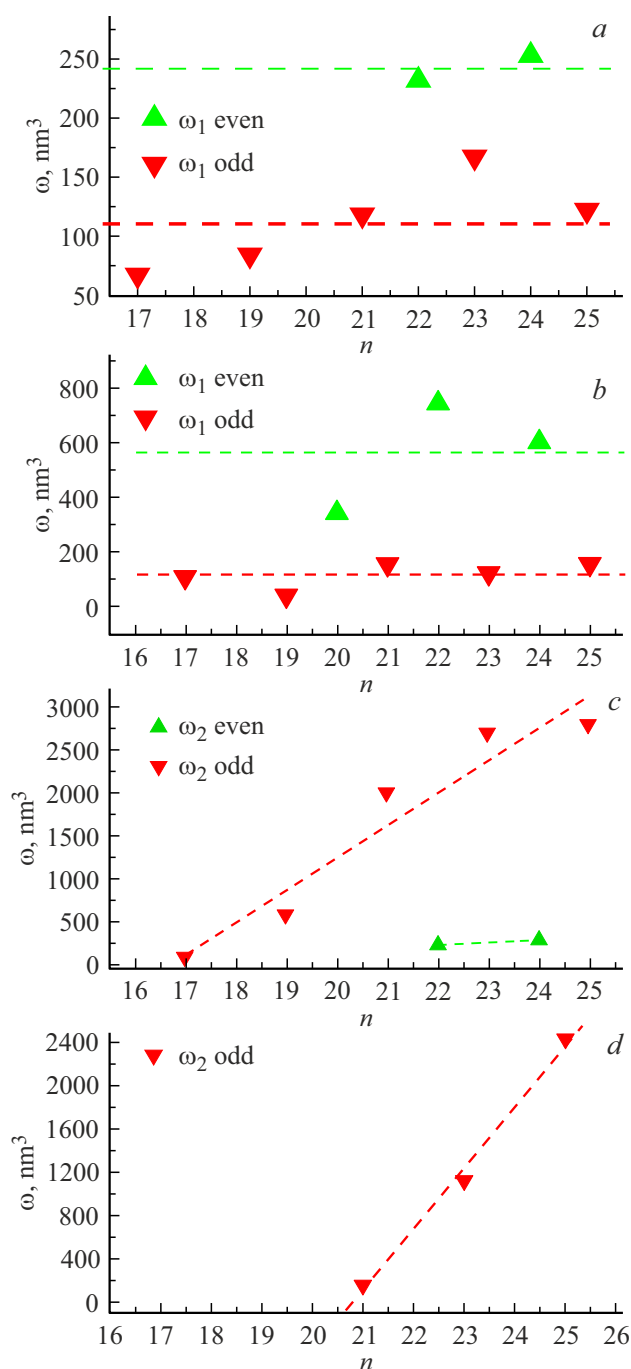


Figure 5. Elementary transformation volumes ω_1 at the first PT-1 stage in heating (a) and in cooling (b) and ω_2 at the second PT-1 stage in heating (c) and in cooling (d).

and, hence, of the number of molecules contained in them (Figure 5, d).

Knowing the nanonuclei volumes ω , nanonuclei approximate thickness may be calculated L , according to [21] for n-alkanes $L = 1.1 \cdot \omega^{1/3}$. Calculation of L for the first stages demonstrating obvious dependence on parity gives $L_{\text{Heven}} = 6.8$ nm and $L_{\text{Hodd}} = 5.3$ nm in heating for even and odd n-alkanes, respectively, and similarly $L_{\text{Ceven}} = 9.1$ nm

and $L_{\text{Codd}} = 5.4$ nm in cooling. The lamella thickness in n-alkanes of the given homologous series does not differ significantly from parity, but, as n grows, varies from 2.2 to 3.4 nm.

Thus, nanonuclei thicknesses of odd n-alkanes coincide in heating and cooling, by comparing their values with lamella thicknesses, it can be established that nanonuclei of odd n-alkanes cover, on average, two lamellae. Nanonuclei thicknesses of even n-alkanes are higher in cooling than in heating. Since change in molecule inclination occurs in structural PT-1 in even n-alkanes, crystallographic cell restructuring process is quite different in heating and cooling. Nanonuclei of even n-alkanes cover two to three lamellae in heating and three to four lamellae in cooling.

3. Conclusion

Analysis of DSC curves performed herein has shown a considerable dependence of thermodynamic parameters of PT-1 on symmetry of n-alkane molecules, while PT-2 parameters did not show such dependence. Examination of development kinetics of heterogeneous PT-1 at the nanolevel using the DPT theory has made it possible to calculate elementary transformation volumes and to identify their dependence on the symmetry of n-alkane molecule. Apparently large nanonuclei volumes in even n-alkanes (~ 2 times greater) are probably explained by more dense cross packaging of molecules in triclinic symmetry crystallographic cells and by more dense packaging of methyl-end groups and, accordingly, by stronger bonds between adjacent lamellae.

The study shows for the first time that the parity effect in the homologous series of n-alkanes caused by the difference in molecule symmetry is in different behavior of several parameters simultaneously such as first-order phase transition temperature, PT-1 temperature hysteresis and elementary transformation volumes of the heterogeneous PT-1. Thus, the parity effect is exhibited not only in the difference of generally observed microscopic PT-1 parameters, but also at the nanolevel, in features of structural transformations of molecular packaging in n-alkanes.

Conflict of interest

The authors declare that they have no conflict of interest.

References

- [1] A. Lazaro, C. Peñalosa, A. Solé, G. Diarce, T. Haussmann, M. Fois, B. Zalba, S. Gshwander, L. Cabeza. *Appl. Energy* **109**, 415 (2013).
- [2] V.M. Egorov, A.K. Borisov, V.A. Marikhin. *Technical Physics Letters* **45**, 12, 1204 (2019).
- [3] D. Cholakova, K. Tsvetkova, S. Tcholakova, N. Denkov. *Colloids Surf. A* **634**, 127926 (2022).
- [4] V.M. Egorov, V.A. Marikhin. *Physics of the Solid State* **58**, 12, 2574 (2016).

- [5] V.M. Egorov, V.A. Marikhin, L.P. Myasnikova, P.N. Yakushev. *Physics of the Solid State* **59**, 10, 2070 (2017).
- [6] Y. Ogawa, N. Nakamura. *Bull. Chem. Soc. Jpn.* **72**, 943 (1999).
- [7] V.M. Egorov, V.A. Marikhin, L.P. Myasnikova. *Polymer Science* **48**, 12, 1270 (2006).
- [8] A.-J. Briard, M. Bouroukba, D. Petitjean, N. Hubert, M. Dirand. *J. Chem. Eng. Data* **48**, 3, 497 (2003).
- [9] V.M. Egorov, V.A. Marikhin, L.P. Myasnikova. *Vysokomolekulyar. soyedineniya* **47B**, 2191 (2005). (in Russian).
- [10] K. Illers. *Eur. Polym. J.* **10**, 911 (1974).
- [11] D.M. Small. *The Physical Chemistry of Lipids*. Plenum Press, N.Y. (1986). 262 p.
- [12] A.E. Chichibabin. *Osnovnye nachala organicheskoy khimii*. Goskhimizdat, M. (1954). V. 1. 795 p. (in Russian).
- [13] S.A. Gureva, A.K. Borisov, V.A. Marikhin, V.M. Egorov. *J. Phys.: Conf. Ser.* **2086P**, 012182 (2021).
- [14] V.M. Egorov, V.A. Marikhin. *Physics of the Solid State* **60**, 7, 1458 (2018).
- [15] T. Yamamoto, K. Nozaki, T. Hara. *J. Phys. Chem.* **92**, 1, 631 (1990).
- [16] S.A. Gureva, V.A. Marikhin, E.N. Vlasova. *Physics of the Solid State* **65**, 12, 2197 (2023).
- [17] G.A. Malygin. *FTT* **36**, 5, 1489 (1994). (in Russian).
- [18] G.A. Malygin. *Physics-Uspexhi*, **44**, 173, (2001).
- [19] M. Fisher. *The Nature of Critical Points*. University of Colorado Press, (1965) 159 p.
- [20] V.M. Egorov, A.K. Borisov, V.A. Marikhin. *Physics of the Solid State* **63**, 3, 498 (2021).
- [21] V.M. Egorov, V.A. Marikhin. *Physics of the Solid State* **58**, 11, 2353 (2016).

Translated by E.Ilinskaya